Passive Q-switching of the Erbium:Glass Laser Using Er^{3+}:CaF_2

Marly B. Camargo,[a] Robert D. Stultz,[b] and Milton Birnbaum
Center for Laser Studies
University of Southern California
DRB 17, University Park
Los Angeles, CA 90089-1112
Tel.: (213) 740-4235, Fax: (213) 740-8158

Abstract

The advantages of passive Q-switching with Er^{3+}:CaF_2, as well as a phenomenological model of the $^4I_{13/2}$ fluorescence decay, are presented.

Key Words

Rare earth doped materials, Fluorescence, Optical properties of materials, Infrared and far-infrared lasers.

Introduction

Eyesafe Er:glass lasers (1.54 μm) are interesting and useful for a large number of applications such as communications, optical atmospheric studies, traffic enforcement, obstacle avoidance, and air defense [1-4]. Many applications require short 1.5 μm pulses with high peak power which can be obtained by Q-switching the Er:glass laser. A saturable absorber Q-switch is the simplest and least expensive Q-switch option, also permitting a very compact resonator size.

Er:glass is a three-level laser where the 1.54 μm transition, $^4I_{13/2} \rightarrow {}^4I_{15/2}$, terminates in the ground-state. Consequently, many Er-doped materials may be used as saturable absorber Q-switches because of the significant overlap of the Er^{3+}:host absorption spectra with the Er:glass emission spectrum.

Er:CaF_2 possesses a broad, continuous absorption spectra nearly coincident with the emission spectrum of Er:glass (Fig. 1). The shorter effective relaxation lifetime of Er:CaF_2 avoids the free-running problems encountered with other Er-doped crystal Q-switches, such as Er^{3+}:$Ca_5(PO_4)_3F$ (or Er:FAP) [5]. The Er:CaF_2 crystals used in these experiments, with 2.0 and 3.5% of Er, were obtained from Optovac, Inc.

Undoped CaF_2 crystals have the cubic structure of fluorite with space group Fm3m [6]. The divalent cations (Ca^{2+}) are at (0,0,0) with the fluorine ions at ±(1/4,1/4,1/4) in an FCC lattice. The presence of Er^{3+}, which replaces the Ca^{2+} ion, distorts the otherwise cubic symmetry due to several possible charge compensation mechanisms, i.e. multiple sites with various crystalline field symmetries are possible. As a result, the optical spectra of Er^{3+} in CaF_2 are complex and characterized by the presence of a large number of overlapping inhomogeneously broadened electronic and/or vibronic lines. The broad (full width at half maximum ≈ 66 nm) absorption band of our (3.5%)Er:CaF_2 crystal with the maximum around 1.54 μm is shown in Fig. 1, along with Er:glass (Kigre QE-7) fluorescence. The absorption spectrum for the (2%)Er:CaF_2 was the same, except the peak absorption coefficient was 2.7 cm^{-1}, instead of 4.4 cm^{-1}.

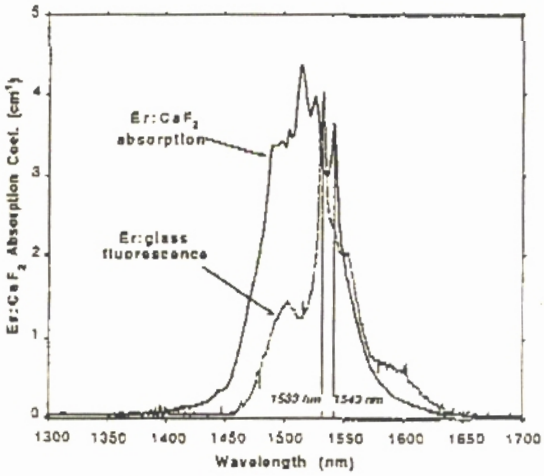

Figure 1. (3.5%)Er:CaF_2 absorption and Er:glass fluorescence.

OSA TOPS on Advanced Solid-State Lasers. 1996
Vol. 1. Stephen A. Payne and Clifford Pollock (eds.)

IPEN-DOC-4737

Spectroscopic Measurements

An Er:glass laser, passively Q-switched with a U:SrF$_2$ saturable absorber Q-switch [7], was used as the excitation source for the lifetime experiments. The laser output energy was 5 mJ and the pulsewidth was 138 ns, full width at half maximum (FWHM). This Q-switched laser had a wavelength of 1533 nm. The Er-crystals were placed near the focus of a +15 cm focal length lens, used to concentrate the laser beam into a 400 μm spot and produce an incident fluence of about 4 J/cm^2.

The crystal fluorescence (Fig. 2) was collected using a fast (f/1.2) glass lens. The light signal was detected by a Ge photodiode (Judson, J16-series). A thin silicon crystal was placed in front of the Ge diode to block possible emissions associated with Er^{3+} energy levels higher than $^4I_{13/2}$.

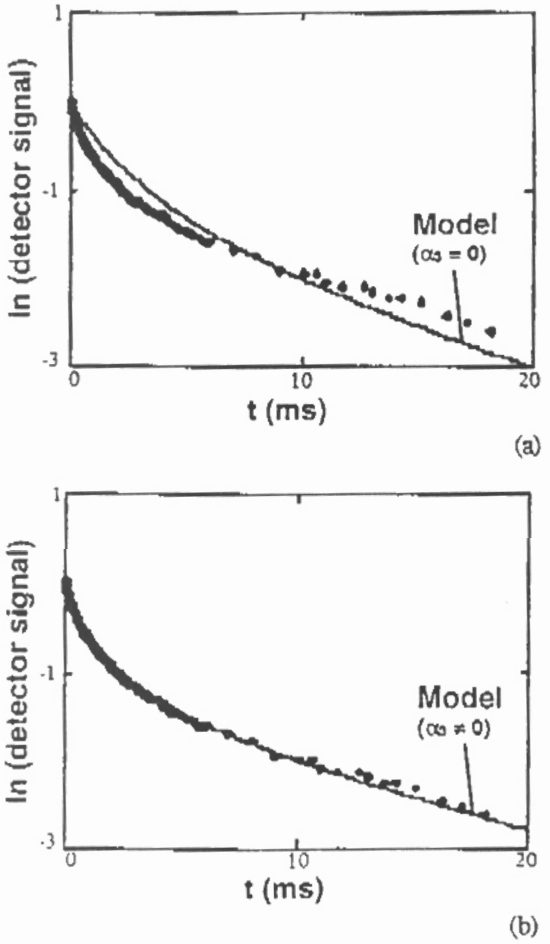

Figure 2. Semi-log plots of (3.5%)Er:CaF$_2$ fluorescence, modeled (a) without cubic term in Eq. (1), and (b) with the cubic term.

Multi-ion processes are strong in Er:CaF$_2$, typically resulting in highly nonexponential $^4I_{13/2}$ fluorescence decays, even with relatively low Er concentrations. Pair theory [8] proved inadequate to model the (3.5%)Er:CaF$_2$ fluorescence (Fig. 2a). Instead, we used the following rate equation for the Er^{3+} $^4I_{13/2}$ population density (m), which includes both quadratic and cubic terms:

$$\frac{dm}{dt} = -\alpha_1 m - \alpha_2 m^2 - \alpha_3 m^3 \tag{1}$$

Using the method of partial fractions, Eq. (1) can be put in the following closed transcendental form:

$$\mu\left(\frac{1+a\mu}{1+a}\right)^{\frac{a}{b-a}}\left(\frac{1+b\mu}{1+b}\right)^{\frac{b}{a-b}} = e^{-\alpha_1 t} \tag{2}$$

where $\mu \equiv m/m_0$, m_0 is the initial ($t = 0$) value of m, and a, b are defined by:

$$a \equiv \frac{F_1 + [F_1^2 - 4F_2\alpha_1]^{0.5}}{2\alpha_1} \tag{3}$$

$$b \equiv \frac{F_1 - [F_1^2 - 4F_2\alpha_1]^{0.5}}{2\alpha_1} \tag{4}$$

where $F_1 \equiv \alpha_2 m_0$, $F_2 \equiv \alpha_3 m_0^2$. We numerically solved Eq. (2), and adjusted the parameters a, b, and α_1 to yield the best fit to the measured (3.5%)Er:CaF$_2$ fluorescence (Fig. 2b). The coefficents used in the model, are given in Table 1.

Table 1. Fluorescence model parameters.

Crystal	m_0	α_1	α_2	α_3
(3.5%) Er:CaF$_2$	~5x10^{18} cm^{-3}	67 s^{-1}	10^{-17} cm^3/s	4x10^{-35} cm^6/s

The absorption cross-section for Er:CaF$_2$ was obtained by bleaching the 2% crystal with a short pulse (14 ns, FWHM) of 1543 nm light from a Raman-shifted Nd:YAG laser, with a spectral linewidth of less than 1 nm. The measured Frantz-Nodvik saturation fluence ($h\nu/\sigma_{eff}$) yielded an effective absorption cross section (σ_{eff}) of 1.43 x 10^{-20} cm^2.

Two Er:CaF$_2$ samples were used to perform the Q-switch experiments: a) 1.0 mm thick piece with 2.0% Er concentration, and b) a 1.1 mm thick piece with 3.5% Er concentration. Both switches were cut and polished with flat and parallel surfaces, and were used uncoated. Since the Er:CaF$_2$ absorption cross-section value is comparable to that of glass, intracavity focusing was necessary to obtain Q-switching [5].

Q-Switched Laser Results and Theory

The Q-switched resonator cavities, all of which possessed stable Gaussian modes, are shown in Fig. 3. The cavity shown in Fig. 3a was flat-flat and with mirror reflectivities of 100% and 88% (outcoupler), at 1533 nm. The length was 21 cm, and a +7.6 cm lens was used to focus the laser beam into the Q-switch. The output mirror in Fig. 3b had a 94% (1533 nm) reflectivity, with a 2.5 cm radius of curvature. The cavity length in this case was 17.5 cm, and a +5 cm intracavity lens was used. Fig. 3c resonator cavity had an internal 2x telescope. All the resonator internal components (except the Q-switches) were AR-coated at 1.54 μm. The Q-switches were always positioned between the output mirror and the intracavity lens, close to the Gaussian beam waist.

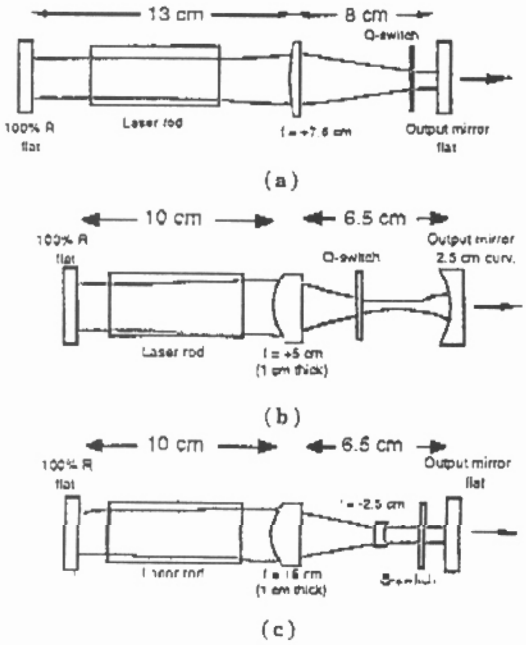

Figure 3. Er:glass resonator cavities.

The Er:CaF$_2$ Q-switch results were obtained using a QE-7S, 3 x 50 mm Er:glass rod, pumped by a Xenon flashlamp with a FWHM pulsewidth of approximately 600 μs. The free-running laser had a threshold of about 14 J with an output slope efficiency of 0.51% for the cavity in Fig. 3b.

The results for both 2% and 3.5% Er:CaF$_2$ Q-switches are summarized in Table 2. The best results were obtained with the (2%)Er:CaF$_2$ switch, using the cavity in Fig. 3b. A typical output pulse obtained is shown in Fig. 4, for this configuration. The Q-switched pulse was recorded using a fast InGaAs photodiode, and the Q-switched output energy was measured using a Scientech calorimeter.

A saturable absorber Q-switch rate equation model was applied to the (2%)Er:CaF$_2$ Q-switch. Using the parameters from Table 2 (losses due to Fresnel reflections from the uncoated surfaces were also included), and the measured value for the absorption cross-section (σ_{ag}), the theoretical model predicted a pulsewidth of 18 ns and an output energy of 36.6 mJ. When the focusing parameter [5], A_g/A_a, was adjusted to 2.94 in the model, the simulated output pulse shape was identical to experiment (see Fig. 4). The corresponding theoretical output energy was 19.3 mJ.

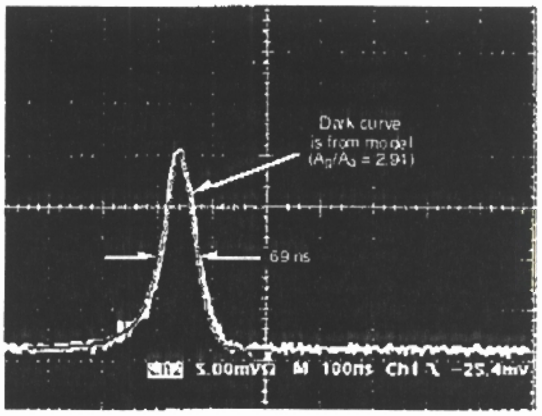

Figure 4. Q-switched pulse.

Conclusion

In conclusion, we have demonstrated a new saturable absorber Q-switch material, Er^{3+}:CaF$_2$, for the 1.54 μm Er:glass laser. We achieved reliable operation with output pulses of 11 mJ, 69 ns in a 17.5 cm laser cavity. The Er:CaF$_2$ did not exhibit any of the free-running problems previously encountered with Er:FAP, because of the rapid initial decay of its $^4I_{13/2}$ level. The theoretical modeling for the Q-switched pulse shapes was in good agreement with experimental data. Further work is required to understand the physical processes involved with the fluorescence decay of the $^4I_{13/2}$ level in this material.

a) *Permanent address: Instituto de Pesquisas Energeticas e Nucleares, CP 11049, CEP 05422-970, S. Paulo, SP, Brazil, Financial support: CNPq/RHAE.*

b) *Permanent address: Hughes Electro-Optical Systems at El Segundo, CA 90245-0902.*

References

1. D. W. Anthon and T. J. Pier, SPIE Proceed. **1627**, 8 (1992).
2. S. E. Sverkov, B. I. Denker, V. V. Osiko, and Yu. E. Sverkov, SPIE Proceed. **1627**, 42 (1992).
3. H. S. Keeter, D. S. Dewald, and M. A. Woodwall, SPIE Proceed. **1627**, 21 (1992).
4. S. J. Hamlin, J. D. Myers, and M. J. Myers, SPIE **1419**, 100 (1991).
5. K. Spariosu, R. D. Stultz, M. Birnbaum, T. H. Allik, and J. A. Hutchinson, Appl. Phys. Lett. **62**, 2763 (1993).
6. R. W. G. Wyckoff, Crystal Structures, Vol. 1, 2nd ed., (Wiley, New York, 1963), Chap. IV, pp. 239-243.
7. R. D. Stultz, M. B. Camargo, S. T. Montgomery, M. Birnbaum, and K. Spariosu, Appl. Phys. Lett. **64**, 948 (1994).
8. R. A. McFarlane, M. Robinson, S. A. Pollack, D. B. Chang, and H. Jenssen, OSA Proceed. on Tunable Solid-State Lasers **5**, 179 (1989).

Table 2. Summary of Er:CaF_2 Q-switched laser experiments.

Q-switch; Thickness (mm)	Resonator cavity; Er:glass rod; Intracavity lens f.l.	Internal transmit. at 1533 nm	A_g/A_s (calc.)	Output mirror reflect. (%)	Output Energy (mJ)	Thresh. (J)	Free-run. output energy (mJ)	Q-sw. pulsewidth (ns)
(2.0%)Er:CaF_2; 1.0	Fig. 3b; 3 x 50 mm QE-7S; +5cm	0.80	12.9	94	11	46	162	69
(2.0%)Er:CaF_2; 1.0	Fig. 3c; 3 x 50 mm QE-7S; +5 & -2.5 cm	0.80	4.0	94	4	35	34	400
(3.5%)Er:CaF_2; 1.1	Fig. 3a; 3 x 50 mm QE-7S; +7.6cm	0.72	6.2	88	3.3	205	not measured	129